The Rip11/Rab11-FIP5 and kinesin II complex regulates endocytic protein recycling

Eric Schonteich[1], Gayle M. Wilson[1], Jemima Burden[2], Colin R. Hopkins[2], Keith Anderson[1], James R. Goldenring[3] and Rytis Prekeris[1,*]

[1]Department of Cellular and Developmental Biology, School of Medicine, University of Colorado Health Sciences Center, 12801 E. 17th Avenue, Aurora, CO 80045, USA
[2]Department of Biological Sciences, Imperial College London, London, SW7 2AZ, UK
[3]Departments of Surgery and Cell and Developmental Biology, Vanderbilt University and the Nashville VA Medical Center, Nashville, TN 37232, USA
*Author for correspondence (e-mail: Rytis.Prekeris@uchsc.edu)

Accepted 1 September 2008
Journal of Cell Science 121, 3824-3833 Published by The Company of Biologists 2008
doi:10.1242/jcs.032441

Summary

Sorting and recycling of endocytosed proteins are required for proper cellular function and growth. Internalized receptors either follow a fast constitutive recycling pathway, returning to the cell surface directly from the early endosomes, or a slow pathway that involves transport via perinuclear recycling endosomes. Slow recycling pathways are thought to play a key role in directing recycling proteins to specific locations on cell surfaces, such as the leading edges of motile cells. These pathways are regulated by various Rab GTPases, such as Rab4 and Rab11. Here we characterize the role of Rip11/FIP5, a known Rab11-binding protein, in regulating endocytic recycling. We use a combination of electron and fluorescent microscopy with siRNA-based protein knockdown to show that Rip11/FIP5 is present at the peripheral endosomes, where it regulates the sorting of internalized receptors to a slow recycling pathway. We also identify kinesin II as a Rip11/FIP5-binding protein and show that it is required for directing endocytosed proteins into the same recycling pathway. Thus, we propose that the Rip11/FIP5-kinesin-II complex has a key role in the routing of internalized receptors through the perinuclear recycling endosomes.

Supplementary material available online at
http://jcs.biologists.org/cgi/content/full/121/22/3824/DC1

Key words: Endosomes, Rab11 GTPase, Kinesin II

Introduction

Eukaryotic cells internalize cell-surface proteins by endocytosis. Endocytosed proteins are first delivered to the multifunctional organelles often referred to as sorting or early endosomes (EE). From there, proteins are either recycled back to the plasma membrane or transported to late endosomes and lysosomes for degradation. Sorting and recycling of endocytosed proteins are required for proper cellular function and growth, yet we still understand little about the mechanisms involved. Quantitative analyses of membrane proteins (such as the transferrin receptor) trafficking through endosomes demonstrate that a variety of alternative pathways exist. Thus, although pulse-chase experiments show that internalized proteins can recycle rapidly (with half-life between 2.5 and 7 minutes), continuous incubations show that longer loading times result in linear, cumulative uptake for up to 40 minutes. Based on these studies, recycling is traditionally divided into 'slow' (perinuclear endosome-dependent) and 'fast' (recycling directly from peripheral endosomes) pathways (Maxfield and McGraw, 2004; Mellman, 1996; Robinson et al., 1996). Although the functional separation between these two recycling pathways remains to be fully understood, it is believed that the fast recycling pathway mediates constitutive protein recycling, whereas the slow recycling pathway mediates a targeted and/or regulated recycling pathway.

Rab 11 GTPase has emerged as an important regulator of endocytic transport (Grosshans et al., 2006; Jordens et al., 2005) and was shown to regulate a slow recycling pathway (Filipeanu et al., 2006; Prekeris, 2003; Ullrich et al., 1996; van der Sluijs et al., 1992; Ward et al., 2005). Accumulating evidence also suggests that Rab11 regulates the polarized recycling of proteins during directional cell migration, cytokinesis and in polarized epithelia (Casanova et al., 1999; Pelissier et al., 2003; Powelka et al., 2004; Skop et al., 2001; Wang et al., 2000; Wilson et al., 2004; Yoon et al., 2005).

Rab GTPases work by recruiting various effector proteins to target membranes. Thus, the recruitment of different effector molecules may be the basis for the involvement of Rab11 in regulating distinct endocytic membrane pathways. Consistent with this idea, several Rab11-interacting proteins have been identified: Rab11BP/Rabphillin-11, Rip11/FIP5, RCP/FIP1, FIP2, FIP3, FIP4, sec15 (exocyst complex subunit) and myosin Vb (Hales et al., 2001; Hales et al., 2002; Hickson et al., 2003; Lindsay et al., 2002; Prekeris et al., 2001; Prekeris et al., 2000; Zhang et al., 2004). All these effectors are grouped in a family of proteins, known as FIPs (Rab11-family-interacting proteins) and are classified into two main classes (Prekeris, 2003; Tarbutton et al., 2005). Class I FIPs (Rip11/FIP5, RCP/FIP1 and FIP2) contain a C2 domain at the N-terminus and interact with Rab11 GTPases in a GTP-dependent manner with an affinity of 50-200 nM (Eathiraj et al., 2006; Junutula et al., 2004). These interactions are mediated by a highly conserved Rab11-binding domain (RBD) situated at the C-terminus of each FIP (Hales et al., 2001; Prekeris et al., 2001).

Rab11-FIP protein complexes appear to work by recruiting additional proteins to endocytic membranes. High-resolution structural analyses of FIP2-Rab11 and FIP3-Rab11 protein complexes show that, upon binding to Rab11 and recruitment to

endocytic membranes, large portions of FIPs become exposed to the cytoplasm in the form of a helical dimer, thus providing the surface for the recruitment of other putative FIP-interacting proteins (Eathiraj et al., 2006; Jagoe et al., 2006; Shiba et al., 2006). In addition, it was shown that different FIPs bind to distinct sets of membrane-traffic-regulating proteins. Thus for instance, Class II FIPs (FIP3 and FIP4) were shown to interact with Arf6 GTPase and the formation of Rab11-FIP3/4-Arf6 complex is required for cell division (Fielding et al., 2005; Shin et al., 2001). Class I FIPs, however, interact with proteins that are known to regulate endocytic membrane recycling in polarized cells, motile fibroblasts and leukocytes (Hales et al., 2002; Naslavsky et al., 2006).

Although recent reports have implicated FIP2 and RCP/FIP1 in regulating various endocytic transport steps, the role of Rip11/FIP5, the third member of the Class I subfamily, remains unclear. Since Rip11/FIP5 is present predominantly in apically localized endosomes in polarized epithelial cells (Prekeris et al., 2000), it is likely that Rip11/FIP5 is also involved in endocytic protein transport and targeting. In this study, we use a combination of electron and fluorescent microscopy with siRNA-based protein knockdown to show that Rip11/FIP5 is present at the peripheral tubular endosomes where it mediates protein sorting to a slow recycling pathway. We also identify kinesin II as a Rip11/FIP5-binding protein. Therefore, we propose that the Rip11/FIP5 and kinesin II protein complex is required for protein sorting to the recycling endosome-mediated slow recycling pathway.

Results

Rip11/FIP5 is localized to peripheral tubular endosomes

Up to now, the localization of Rip11/FIP5 in non-polarized cells has not been properly investigated. We therefore determined the localization of Rip11/FIP5 by staining HeLa cells with antibodies against Rip11/FIP5 and various endocytic markers, such as Lamp1 (late endosomes/lysosomes), Golgin-97 (trans-Golgi network, TGN) and EEA1 (early endosomes). Rip11/FIP5 did not colocalize with any of these markers (data not shown), a finding consistent with published work showing that Rip11/FIP5 is recruited to endosomes by binding to Rab11, a GTPase enriched in perinuclear recycling endosomes and tubular extensions of early endosomes (Junutula et al., 2004). To explore this further we treated HeLa cells with antibodies against Rip11/FIP5 and the transferrin receptor (TfR). As shown in Fig. 1A-F, Rip11/FIP5 partially colocalized with TfR. However, although some TfR-containing endosomes also stained for Rip11/FIP5 (Fig. 1D-F, arrowheads), a significant number of TfR-containing endosomes did not contain detectable Rip11/FIP5. Overall colocalization was modest, with only 22±4.3% of TfR endosomes overlapping with Rip11/FIP5. By contrast, 76.3±8.2% of Rip11/FIP5-containing organelles were also positive for TfR. Interestingly, Rip11/FIP5 was often enriched on the subdomains of larger TfR-containing endosomes (Fig. 1D-F, arrows). These data suggest that Rip11/FIP5 may regulate transport only in a distinct subset of the TfR-containing endosomes.

To investigate Rip11/FIP5 localization further, we loaded HeLa cells with Tf-HRP conjugate (for 45 minutes at 37°C) and analyzed Rip11/FIP5 localization (Rip11/FIP5 was labeled with 10 nm immunogold) using electron microscopy (Fig. 1G,H). Most of the Rip11/FIP5 label was localized to tubular endosomes containing TfR (identified by the electron-dense precipitate of the reaction product derived from HRP activity). Some Rip11/FIP5 could be observed clustered on the subdomains of Tf-HRP-containing endosomes. Consistent with immunofluorescence microscopy, very little Rip11/FIP5 labeling could be found on late endosomes (see inset in Fig. 1G) or lysosomes (data not shown).

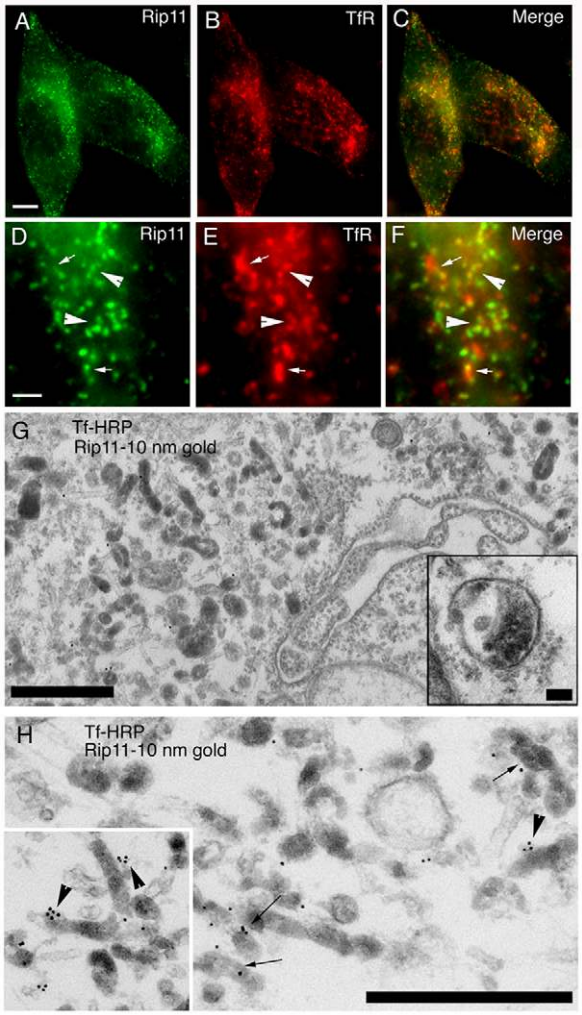

Fig. 1. Rip11/FIP5 is enriched in peripheral recycling endosomes. (A-F) HeLa cells were plated on collagen-coated glass coverslips fixed and stained with anti-TfR (B,C,E,F, red) or anti-Rip11/FIP5 (A,C,D,F, green) antibodies. Yellow in C and F represents overlap between TfR and Rip11/FIP5. (D-F) High-magnification images of the same cell. Arrowheads in D-F indicate organelles where TfR and Rip11 colocalize. Arrows in D-F indicate organelles where Rip11/FIP5 is enriched in subdomains. Scale bars: 5 μm (A) and 1 μm (D). (G,H) HeLa cells were incubated with transferrin-HRP for 45 minutes at 37°C before being processed for immunoelectron microscopy. Anti-Rip11/FIP5 antibodies were detected using 10 nm gold. The electron-dense DAB reaction product indicates the presence of Tf. Clusters of Tf-positive endosomes that are also positive for Rip11/FIP5 are visible. Scale bars: 500 nm. Inset in H is a higher magnification image of endocytic tubules. Inset in G shows a vesicular part of an early endosome that is negative for anti-Rip11/FIP5 antibodies. Scale bar: 100 nm. Arrows indicate Tf-HRP-containing endosomes that are also positive for Rip11-gold. Arrowheads indicate Rip11 clusters on Tf-HRP endosomes.

Rip11/FIP5 mediates the transport of TfR to the slow recycling pathway

Next, we used siRNA-dependent Rip11/FIP5 knockdown to measure TfR endocytic traffic in HeLa cells. To eliminate the possibility of the off-target effects, most experiments were confirmed using two different Rip11/FIP5 siRNAs (supplementary

material Fig. S1). Initially we measured the uptake of Tf–Alexa-Fluor-488 (Tf-Alexa488) in mock-transfected cells or in cells transfected with Rip11/FIP5 siRNA. Consistent with our previous reports, Rip11/FIP5 knockdown resulted in a significant increase in Tf internalization (Fig. 2A) compared with the knockdown of RCP/FIP1, which resulted in the inhibition of Tf uptake (Peden et al., 2004). By contrast, lysosomal degradation of BSA and internalization of EGF receptor (EGF-R) were not affected (supplementary material Fig. S3). Increase in Tf uptake can be caused by changes in cellular TfR levels, or changes in rates of internalization and/or recycling. As shown in Fig. 2B (see also supplementary material Figs S1 and S2), Rip11/FIP5 knockdown increased plasma membrane levels of TfR, but it had no effect on total cellular TfR levels. The increase was specific to actively recycling proteins, because plasma membrane levels of epidermal growth factor receptor (EGFR) were not affected by Rip11/FIP5 depletion (supplementary material Fig. S3). Furthermore, although Rip11/FIP5 knockdown had no effect on the half-life of Tf internalization and recycling (Fig. 2A,C,D), Rip11/FIP5 knockdown increased the amount of Tf uptake and recycling (Fig. 2C,D). In summary, these data suggest that Rip11/FIP5 depletion results in an increase in the number of TfRs in the rapidly recycling endocytic carriers, thus increasing the amount of Tf internalized and recycled.

To confirm that Rip11/FIP5 regulates the number of TfRs actively reccycling between the endocytic compartment and the plasma membrane, we tested the effect of Rip11/FIP5 siRNA knockdown on the relative distributions of Tf-Alexa594 (loaded at 37°C for 30 minutes) and anti-TfR antibodies. As shown in Fig. 3A-F, in mock-transfected cells only 68.3±3.8% of TfR colocalized with Tf-Alexa594. By contrast, almost 100% of Tf-Alexa594 colocalized with TfR, although the ratio between Tf-Alexa594 and TfR levels varied considerably between different endosomes (Fig. 3A-F). These data suggest that a subpopulation of TfR does not actively recycle to the plasma membrane, probably representing the previously described ‘slow’ recycling pool. To test whether Rip11/FIP5 regulates the transport of TfR between slow and fast recycling pools, we analyzed Tf-Alexa594 and TfR colocalization in HeLa cells treated with Rip11/FIP5 siRNA. As shown in Fig. 3G-L, Rip11/FIP5 knockdown increased the colocalization between TfR and Tf-Alexa594 to 81.2±3.4% (significantly different from control at $P<0.05$).

It is noteworthy that Rip11/FIP5 knockdown also resulted in accumulation of TfR in large organelles that could represent early endosomes. To test this, we incubated mock-transfected or Rip11/FIP5 siRNA-treated cells with Tf-Alexa488 for 30 minutes at 37°C and analyzed its colocalization with the early endosome marker EEA1. As shown in Fig. 4A-C, after a 30 minute incubation, the majority of Tf-Alexa488 was present in perinuclear recycling endosomes, with some Tf-Alexa488 also present at the tips of the

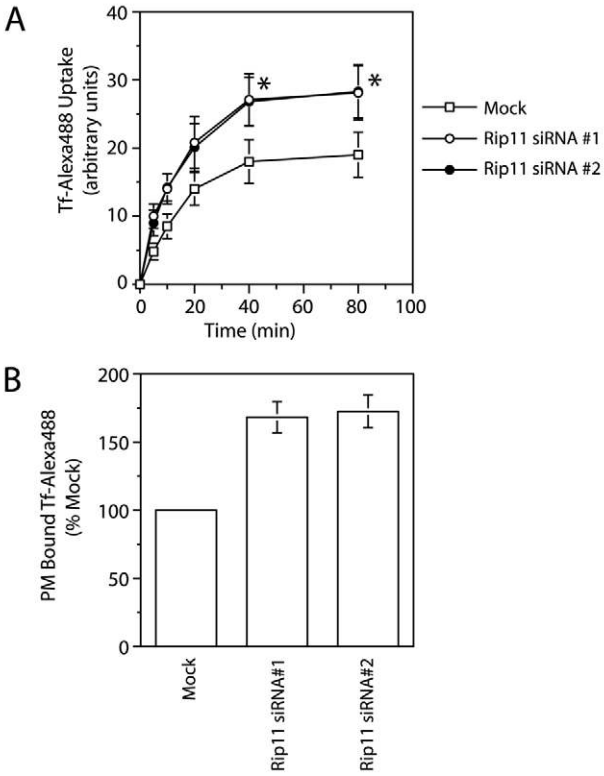

D

	Mock	Rip11 siRNA#1	Mock	Rip11 siRNA#1
	T1/2 (min)		Arbitrary fluorescence units/min (first 20 min)	
Uptake	12.3+/-2.1	12.5+/-1.8	0.63+/-0.2	1.11+/-0.2*
Recycling	9.6+/-3.4	11.2+/-3.2	1.1+/-0.3	1.9+/-0.2*

Fig. 2. Rip11/FIP5 knockdown increases Tf uptake. (A) HeLa cells treated with mock siRNA, Rip11/FIP5 siRNA1 or Rip11/FIP5 siRNA2 were incubated at 37°C with Tf-Alexa488. Cells were then washed, fixed and internalized Tf-Alexa488 measured by flow cytometry. The data shown are the mean ± s.d. of three independent experiments. Asterisks indicate time points that are significantly different from mock-treated control at $P<0.025$. (B) Mock-treated or Rip11/FIP5 siRNA-treated HeLa cells were fixed and incubated with 80 μg/ml Tf-Alexa488 in the absence or presence of 0.4% saponin. Cells were then washed and plasma-membrane-associated (non-permeabilized cells, see figure) and total cellular (permeabilized cells, not shown) Tf-Alexa488 measured by flow cytometry. The data shown are the mean ± s.d. of three independent experiments. (C) Mock- and Rip11/FIP5 siRNA1-treated HeLa cells were incubated at 37°C for 30 minutes with Tf-Alexa488. Cells were then washed and incubated at 37°C with unlabeled Tf. Cell-associated Tf-Alexa488 was measured by flow cytometry and is shown as arbitrary units. The data shown are the mean ± s.d. of three independent experiments. *$P<0.01$. (D) The rates of Tf uptake and recycling calculated from the data presented in A and C. The data shown are the half-life of uptake and recycling (T1/2) as well as the amount of Tf-Alexa488 internalized and recycled (arbitrary fluorescence units per minute). Data are the mean ± s.d. calculated from three different experiments. *$P<0.02$.

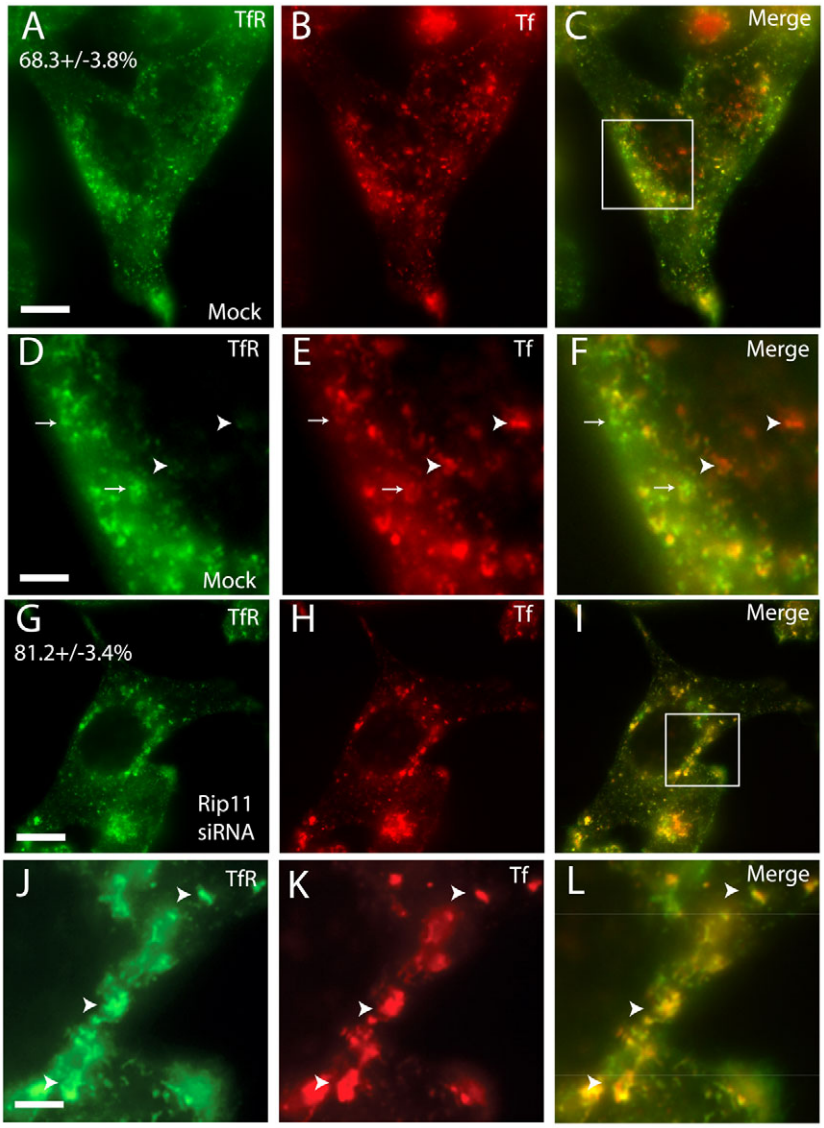

Fig. 3. Rip11/FIP5 knockdown increases colocalization of Tf with TfR. Mock-treated (A-F) or Rip11 siRNA1-treated (J-L) HeLa cells were loaded for 30 minutes at 37°C with 5 μg/ml Tf-Alexa594 (B,C,E,F,H,I,K,L, red). Cells were then washed fixed and stained with anti-TfR antibodies (A,C,D,F,G,I,J,L, green). Yellow in C,F,I and L represents the overlap between Tf-Alexa594 and TfR. D-F and J-L are higher magnification images of boxed areas of mock-treated and Kif3B siRNA1-treated cells, respectively. Scale bars: 5 μm (A,G) and 1 μm (D,J). Arrowheads in D-F indicate organelles enriched in Tf-Alexa594. Arrows in D-F indicate organelles containing TfR but little Tf-Alexa594. Arrowheads in J-L point to large organelles enriched in TfR and Tf-Alexa594. Numbers in A and G give the percentage overlap between TfR and Tf-Alexa594. The data are mean ± s.d. overlap in 25 randomly chosen cells from three different experiments.

cells. Only a small portion of Tf-Alexa488 (11.2±1.2%) was present in early endosomes, as shown by partial colocalization with EEA1. The Rip11/FIP5 knockdown caused a decrease in Tf-Alexa488 localization in perinuclear recycling endosomes and an increase in colocalization of Tf-Alexa488 and EEA1 (Fig. 4D-F) (35.3±2.8%). Interestingly, in Rip11/FIP5-knockdown cells, the amount of Tf-Alexa488 present at the tips of the cells did not seem to change (Fig. 4D-F). Since these organelles did not stain with anti-EEA1 antibody, they are unlikely to be early endosomes, suggesting that Rip11/FIP5 knockdown has not completely blocked the exit of Tf from early endosomes, but does, probably, affect the transfer of Tf from early endosomes to the perinuclear recycling endosomes.

Kinesin II is a Rip11/FIP5-binding protein

To discover new Rip11/FIP5-binding proteins we screened a human kidney cDNA library using a yeast two-hybrid assay. Five clones isolated during this screen encoded the C-terminal fragments of Kif3B, a component of the kinesin II molecular motor. Kinesin II is a microtubule molecular motor that consists of a Kif3A and Kif3B heterodimer that is associated with a single molecule of KAP3A (Cole et al., 1992; Cole et al., 1993). All isolated Kif3B clones included the C-terminal tail domain, which is thought to mediate kinesin-cargo interactions. Thus, we tested whether Kif3B(524-747) (Kif3B-tail) can bind to Rip11/FIP5. As shown in the supplementary material Fig. S6A, Rip11/FIP5 but not RCP/FIP1 interacted with Kif3B-tail. Interestingly, no binding was observed to KAP3A, suggesting that Rip11/FIP5 binds directly to Kif3B rather than through KAP3 (supplementary material Fig. S6A), has been reported for some other kinesin II cargo molecules (Jimbo et al., 2002; Takeda et al., 2000).

Next, we evaluated whether Rab11 regulates Rip11/FIP5 binding to Kif3B. To this end we tested the Rip11/FIP5-Y629A mutant for its ability to bind Kif3B-tail. We have previously reported that Rip11/FIP5-Y629 plays a key role in its binding to Rab11 (Junutula et al., 2004). The Rip11/FIP5-Y629A mutant still bound to the Kif3B-tail as tested by a yeast two-hybrid assay (supplementary material Fig. S6B). Although Rab11 did not seem to affect Rip11/FIP5 binding to Kif3B, it is still possible that Rab11 might bind to either Kif3B or KAP3, thus increasing the specificity and/or affinity of Rip11/FIP5-Rab11 complex interaction with kinesin II. We then tested whether Rab11 could independently bind to Kif3B or KAP3, but neither wild-type Rab11 nor Rab11 mutants (dominant-negative or constitutively active) interacted with Kif3B or KAP3 (supplementary material Fig. S6C).

In vivo, kinesin II exists as a heterotrimeric protein complex consisting of Kif3A-Kif3C-KAP3 or Kif3A-Kif3B-KAP3 proteins. Thus, we tested whether Rip11/FIP5 can bind all three Kif3 isoforms. Rip11/FIP5 bound to GST-Kif3A, B and C, but not GST alone (Fig. 5A,B). To identify the Kif3B-binding domain in Rip11/FIP5, we purified the Rip11/FIP5(490-652) fragment that was previously shown to contain the Rab11-binding domain (Meyers and Prekeris, 2002; Junutula et al., 2004). Consistent with yeast two-hybrid data, Rip11/FIP5(490-652) bound to GST-Kif3B-tail, but not GST alone (Fig. 5C). Furthermore, addition of excess soluble wild-type Rab11 did not affect Rip11/FIP5 and Kif3B-tail binding (Fig. 5C), suggesting that Rab11 and Kif3B bind to distinct and non-overlapping sites. Consistent with this, constitutively active Rab11 (Q70L) or dominant-negative Rab11 (S25N) had no effect on Rip11/FIP5 binding to GST-Kif3B-tail (data not shown). Rab11

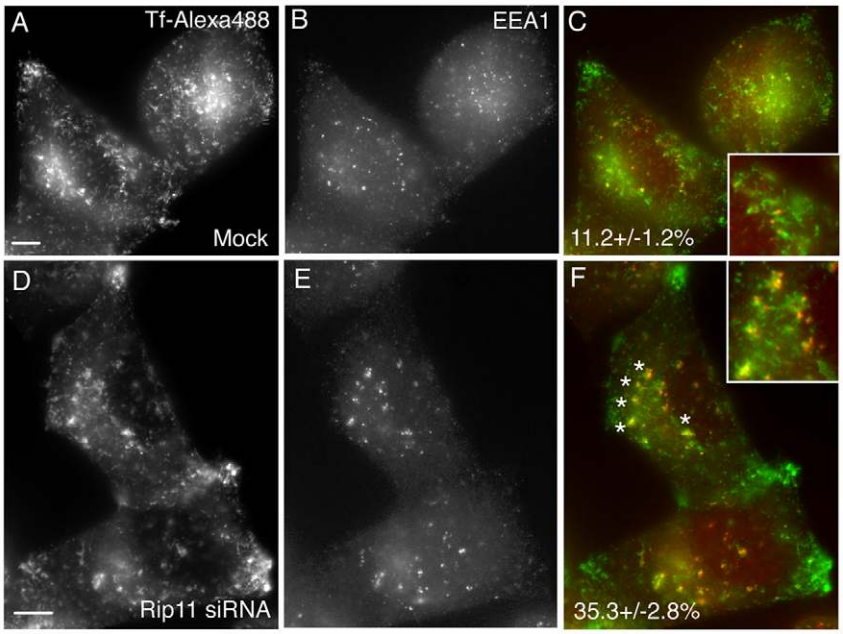

Fig. 4. Rip11/FIP5 knockdown increases colocalization of Tf with early endosomes. Mock-treated (A-C) or Rip11 siRNA1-treated (D-F) HeLa cells were incubated for 30 minutes with Tf-Alexa488 (A,D and green in C,F). Cells were then washed, fixed and stained with anti-EEA1 antibody (B,E and red in C,F). Yellow colour represents the extent of Tf and EEA1 overlap. Asterisks indicate early endosomes. Insets in C and F are higher magnification images. Numbers in C and F represent the extent of colocalization of Tf-Alexa488 with EEA1. The numbers are the mean ± s.d. from ten random cells. Scale bars: 4 μm.

was also pulled down with GST-Kif3B beads, but only in the presence of Rip11/FIP5(490-652) (Fig. 5C and data not shown) suggesting that Rip11/FIP5 and Rab11 complex can bind to Kif3B.

Kif3B mediates Rip11/FIP5 binding to microtubules

Accumulating evidence suggests that microtubule-dependent motors have an important role in endocytic protein trafficking (Soldati and Schliwa, 2006) and it is of interest therefore that Rip11/FIP5-containing endosomes can often be observed aligned in a 'beads-on-a-string' manner along microtubules (supplementary material Fig. S4). To test whether kinesin II mediates recruitment of Rip11/FIP5 to microtubules, we examined the ability of Rip11/FIP5 to bind microtubules by in vitro microtubule sedimentation assays. As shown in Fig. 5D, endogenous Rip11/FIP5 from HeLa Triton X-100 lysates could be sedimented with microtubules. This interaction was not direct, because recombinant purified Rip11/FIP5 did not co-sediment with microtubules (data not shown). To test whether molecular motor proteins mediate this interaction, we incubated HeLa cell lysates solubilized with Triton X-100, with microtubules in the presence of 5 mM ATP, which is known to dissociate molecular motors from microtubules. ATP decreased Rip11/FIP5 co-sedimentation with microtubules (Fig. 5E). To test whether molecular motors recruit Rip11/FIP5 to microtubules, we incubated HeLa cells lysates with microtubules in the absence of ATP, sedimented tubulin and then resuspended and re-sedimented microtubules in the absence or presence of 5 mM ATP (Fig. 5E, top panel, last two lanes). Once again, ATP inhibited Rip11/FIP5 re-sedimentation with microtubules.

The ATP effect on Rip11/FIP5 co-sedimentation with microtubules suggests that molecular motors, such as kinesins, mediate the Rip11/FIP5 interaction with tubulin. However, this assay does not determine the identity of this kinesin. To test whether kinesin II mediates Rip11/FIP5 co-sedimentation with microtubules, we performed the assay either in the presence or absence of recombinant purified Kif3B-tail protein or using Triton X-100 lysates from HeLa cells treated with Kif3B siRNA. In both cases, we observed a decrease in Rip11/FIP5 co-sedimentation with microtubules, suggesting that kinesin II is required for Rip11/FIP5 binding to microtubules (Fig. 5E).

Kinesin II regulates protein traffic to perinuclear recycling endosomes

Our data suggest that kinesin II binding to Rip11/FIP5 might be involved in regulating protein transport to perinuclear recycling endosomes. Although kinesin II has a well-established role in primary cilia generation and maintenance in epithelial cells, as well as lysosomal transport, its role in endocytic recycling remains obscure (Bananis et al., 2004; Brown et al., 2005; Lin et al., 2003; Soldati and Schliwa, 2006; Whitehead et al., 1999). To this end, we developed two different Kif3B siRNAs, siRNA1 and siRNA2 that resulted in 80% and 70% knockdown of Kif3B, respectively (supplementary material Fig. S1A,C). Interestingly, the knockdown of Kif3B also caused the depletion of Kif3A (the antibody recognizes both kinesin II subunits), but not KAP3A (supplementary material Fig. S1A-C). Since Kif3B siRNA1 more efficiently knocked down Kif3A/B, we used it for most of the following experiments. However, to avoid off-target effects, most of the experiments were repeated at least once with Kif3B siRNA2 (data not shown).

First, we tested the uptake of Tf-Alexa488 (to analyze recycling pathways) as well as the uptake of DQ-BSA-Green (to analyze lysosomal degradation pathways). Similarly to results with Rip11/FIP5 siRNA, Kif3B knockdown resulted in increased Tf-Alexa488 internalization (Fig. 6A,C), but had no effect on DQ-BSA-Green transport to lysosomes (supplementary material Fig. S3). Kif3B depletion increased the amount of Tf-Alexa488 uptake and recycling (Fig. 6A,C), but had no effect on the half-life of Tf-Alexa488 recycling (data not shown). Furthermore, Kif3B depletion resulted in an increase in plasma membrane levels of TfR (Fig. 6B).

To understand the role of kinesin II in protein recycling, we incubated Kif3B siRNA1-treated HeLa cells with Tf-Alexa488. Similarly to Rip11/FIP5 knockdown, treatment of HeLa cells with Kif3B siRNA resulted in the loss of the tubulated Tf-Alexa488 structures in the cytoplasm (Fig. 7A). Surprisingly, although a small

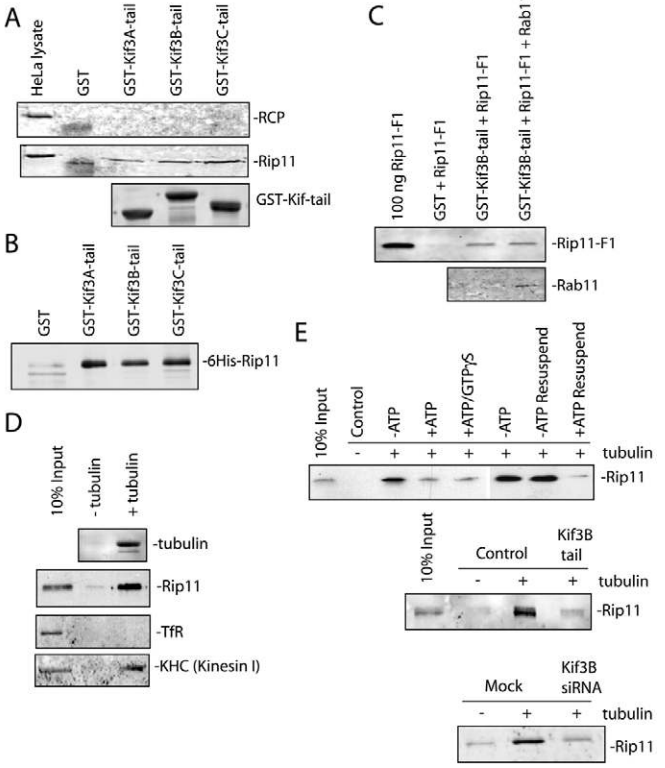

Fig. 5. Kinesin II mediates Rip11/FIP5 binding to microtubules. (A) Glutathione beads coated with GST alone, GST-Kif3A-tail, GST-Kif3B-tail or GST-Kif3C-tail were incubated with HeLa cell Triton X-100 lysates. Beads were then washed and bound Rip11/FIP5 or RCP/FIP1 was analyzed by immunoblotting. The lower molecular size band present only in the GST lane represents a non-specific band since it did not disappear when we use lysates treated with Rip11/FIP5 siRNA (data not shown). (B) Glutathione beads coated with GST alone, GST-Kif3A-tail, GST-Kif3B-tail or GST-Kif3C-tail were incubated with recombinant purified 6His-Rip11/FIP5. Bound 6His-Rip11/FIP5 was detected by immunoblotting. (C) Glutathione beads coated with either GST alone or GST-Kif3B-tail were incubated with Rip11/FIP5(490-652) in the presence or absence of recombinant Rab11a. Bound Rip11/FIP5(490-652) was detected by immunoblotting. (D,E) Rip11/FIP5 binding to microtubules analyzed using microtubule sedimentation assay (see Materials and Methods). Where indicated, assays were performed in the presence off either 5 mM ATP or recombinant Kif3B-tail protein. In the bottom panel, mock-treated or Kif3B siRNA-treated lysates were used in the assay.

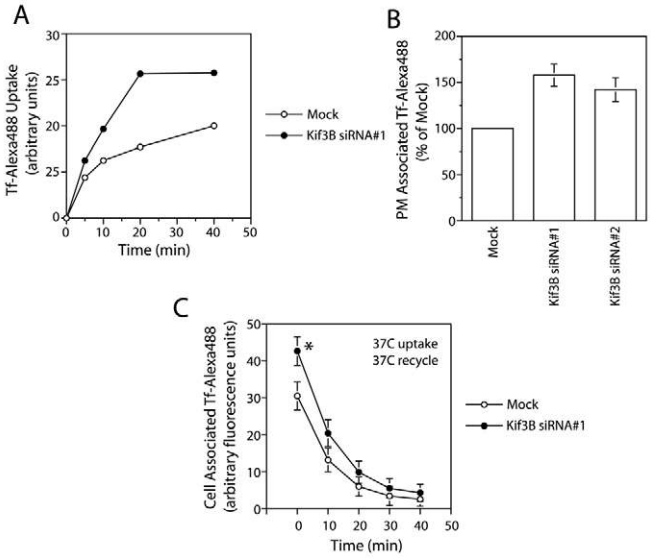

Fig. 6. Kif3B knockdown increases Tf uptake. (A) Mock-treated or Kif3B siRNA1-treated HeLa cells incubated at 37°C with Tf-Alexa488. Internalized Tf-Alexa488 was measured by flow cytometry. The data shown are the means of two independent experiments. (B) Mock-treated or Kif3B siRNA-treated HeLa cells were fixed with 4% paraformaldehyde and incubated with 80 μg/ml of Tf-Alexa488 in the absence of saponin. Plasma-membrane-associated Tf-Alexa488 was measured by flow cytometry. The data shown are the means ± s.d. of three independent experiments. (C) Mock-treated or Kif3B siRNA1-treated HeLa cells incubated at 37°C for 30 minutes with Tf-Alexa488. Cells were incubated with unlabeled Tf. Cell-associated Tf-Alexa488 was then measured by flow cytometry and is shown as arbitrary fluorescence units. The data shown are the mean ± s.d. of three independent experiments. *P<0.025.

fraction of Tf-Alexa488 could be found in EEA1-containing early endosomes (Fig. 7A-C, inset), the majority of Tf-Alexa488 was present in the endocytic structures located at the tips of the cells (Fig. 7A-C). These structures also contained other endocytic proteins, such as Rab11, Rab4, RCP/FIP1, FIP2 and Rip11/FIP5 (data not shown and supplementary material Fig. S5), but not lysosomal or TGN markers, such as Lamp1, VAMP7 and Golgin97. In addition, these organelles are still able to recycle Tf, because Tf-Alexa488 can be chased out of them (supplementary material Fig. S5D,E). All these data suggest that these elements probably belong to the slow perinuclear recycling compartment that is usually observed next to the nucleus.

To further understand the role of kinesin II and Rip11/FIP5 in endocytic recycling, we treated HeLa cells with both Kif3B and Rip11/FIP5 siRNAs. Knockdown of Kif3B and Rip11/FIP5 (for the efficiency of knockdown see supplementary material Fig. S1) resulted in partial shift of Tf-Alexa488 from cell tips to cytoplasmic structures (Fig. 8C,E compare with Fig. 8A,B) that also contained EEA1 (data not shown). This phenotype is similar to that observed with Rip11/FIP5 knockdown alone, suggesting that although Rip11/FIP5 and kinesin II act in the same recycling pathway, Rip11/FIP5 might have additional functions upstream of kinesin II. Indeed, it has been suggested that FIPs also regulate membrane transport by interacting with multiple proteins in a 'hand-me-down' fashion.

Discussion

A key step in understanding endocytic traffic is the characterization of the role that Rab GTPases and their effector proteins have in regulating protein transport and sorting. Rip11/FIP5 was originally identified as a Rab11-binding protein that is enriched at the apical recycling endosomes in polarized epithelial cells (Prekeris et al., 2000). Since then, it has become apparent that, although Rip11/FIP5 is enriched in polarized epithelial cells, it is present in all other cell lines or tissues tested (Junutula et al., 2004; Peden et al., 2004; Prekeris et al., 2000). Thus, it is likely that Rip11/FIP5 function is not limited to endocytic membrane traffic in epithelial cells. Here we show that in non-polarized HeLa cells, Rip11/FIP5 associates with peripheral tubular endosomes. It is interesting to note that Rip11/FIP5 can often be observed localized in clusters associated with 'bud-like' structures on the endosomes. It is tempting to speculate that these structures could be the sites of budding transport vesicles or tubules. Consistent with this, Rab11 GTPases are enriched in clathrin-coated vesicles (Borner et al., 2006). Furthermore, overexpression of Rip11/FIP5 dominant-negative

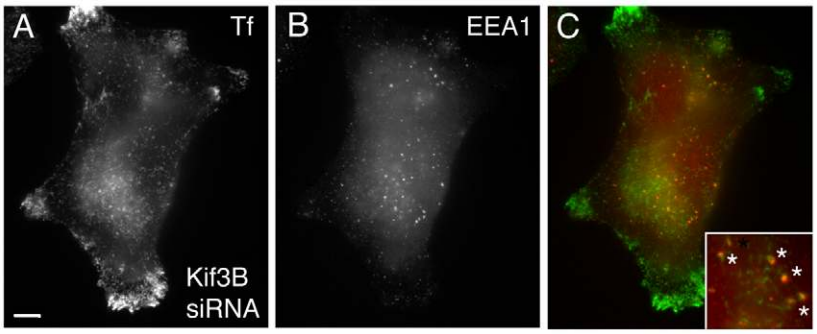

Fig. 7. Kif3B knockdown results in peripheral accumulation of TfR. (A-C) Kif3B siRNA1-treated cells incubated for 30 minutes with Tf-Alexa488 (A,C, green). Cells were then fixed and stained with anti-EEA1 antibodies (B,C, red). Asterisks in inset in C indicate the early endosomes containing Tf. Yellow in C represents the overlap between Tf-Alexa488 and EEA1. Scale bar: 5 μm.

mutant causes extensive tubulation of recycling endosomes (Junutula et al., 2004; Meyers and Prekeris, 2002), suggesting a defect in budding from tubular endosomes. However, whether Rip11/FIP5 is simply recruited to the budding sites or actively regulates transport vesicle/tubule formation remains to be determined.

Perhaps the most intriguing observation is that Rip11/FIP5 knockdown actually enhances Tf uptake, rather than inhibiting it. The enhancement in Tf uptake was mostly due to the increase in the amount of TfR present in actively recycling endocytic carriers, rather then changes in the half-life of endocytosis or recycling. Consistent with this, Rip11/FIP5 knockdown increases the amount of TfR at plasma membrane. Furthermore, it also inhibits TfR transfer from early endosomes to perinuclear recycling endosomes. These data suggest that Rip11/FIP5 mediates perinuclear slow recycling rather than constitutive fast recycling. The functional significance of slow recycling remains to be clarified. The perinuclear recycling endosome is a very heterogeneous compartment that may well contain several functionally distinct endosome components. It is likely that recycling through the different subcompartments of recycling endosomes is used for specialized or targeted recycling pathways. Indeed, in polarized epithelial cells, a subset of recycling endosomes, also known as apical recycling endosomes (AREs), mediates apical protein targeting (Hoekstra et al., 2004). Furthermore, Rab11 and Rip11/FIP5 mediate apical transport through such AREs (Casanova et al., 1999; Nedvetsky et al., 2007; Prekeris et al., 2000; Wang et al., 2000). Similarly, migrating cells produce lamellipodia at their leading edges and the additional membrane-targeted Rab11-dependent delivery of integrins required for these protrusive processes is thought to be derived from the recycling endosomes (Powelka et al., 2004; Yoon et al., 2005). Thus, Rip11/FIP5 might have a key role in promoting the transfer of trafficking proteins away from constitutive fast to the regulated or targeted slow recycling pathway.

Several recent reports suggest that once recruited to the endosomes by binding to Rab11, FIPs function as scaffolding factors or adaptor molecules that recruit various proteins that regulate membrane transport. Since Rab11 forms mutually exclusive

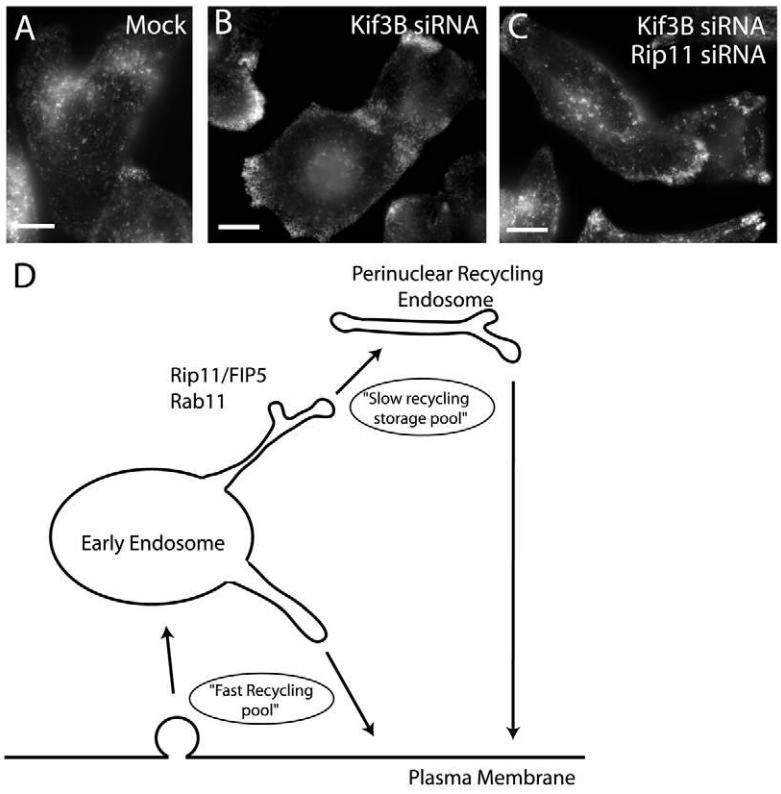

Fig. 8. Rip11/FIP5 and Kif3B regulate the same recycling pathway. (A-C) Mock-treated cells (A) or cells treated with Kif3B siRNA1 (B) or Kif3B and Rip11/FIP5 siRNA1 (C) were incubated at 37°C for 30 minutes with Tf-Alexa488. Scale bars: 5 μm. (D) Proposed model of roles of Rip11/FIP5 and kinesin II in mediating transport to the slow storage pool of endocytic recycling.

complexes with various FIPs, different FIP-Rab11 complexes could mediate distinct membrane transport pathways. Indeed, in the past few years several proteins that interact specifically with different members of the FIP family have been identified (Fielding et al., 2005; Hales et al., 2002; Naslavsky et al., 2006). In this study we identified kinesin II as a molecular motor that binds to Rip11/FIP5. We originally identified kinesin II as a putative Rip11/FIP5-binding protein by yeast two-hybrid assays and confirmed the binding using glutathione pull-down assays, as well as microtubule co-sedimentation assays. Unfortunately, we could not demonstrate co-immunoprecipitation of kinesin II and Rip11/FIP5 using either anti-Rip11 or anti-GFP (in Rip11-GFP-expressing cells) antibodies. It is possible that the interaction between Rip11/FIP3 and kinesin II is either too transient or not strong enough to withstand the immunoprecipitation. Alternatively, microtubule binding might be required to enhance the kinesin II interaction with Rip11/FIP5. Several studies have shown that kinesins can auto-inhibit their cargo binding when not associated with microtubules (Blasius et al., 2007), usually through the motor head group interacting with the cargo-binding tail domain. Consistent with this, in yeast two-hybrid assays, the tail domain of Kif3B bound to Rip11 more strongly than full-length Kif3B (data not shown).

Kinesin II is a well-studied microtubule molecular motor that mediates various cellular processes, including primary cilia formation and maintenance, late endosome transport and cytokinesis (Brown et al., 2005; Fan and Beck, 2004; Haraguchi et al., 2006; Jimbo et al., 2002; Whitehead et al., 1999). Kinesin II is a heterotrimer that consists of two heavy chains, Kif3B and Kif3A, and a single light chain KAP3. Kinesin II binds to Rip11/FIP5 via the tail domains of Kif3B and Kif3A subunits. KAP3 does not mediate Rip11/FIP5 binding, although we cannot rule out the possibility that it regulates Rip11/FIP5 and Kif3A/B interactions in vivo by binding to the tail domains of Kif3A/B. Indeed, kinesin II might transport different cargoes by binding either to cargo via KAP3 or directly to the tails of Kif3A/B.

The interaction between Rip11/FIP5 and Kif3A/B suggested that kinesin II is involved in endocytic protein transport. Consistent with this, Kif3B knockdown resulted in an increase in the amount of actively recycling TfR while having little effect on the half-life of endocytosis or recycling. Surprisingly, although Rip11/FIP5 knockdown resulted in the increased association of TfR with early endosomes, Kif3B knockdown caused an accumulation of endosomes at the tips of cells, suggesting that kinesin II has additional functions in regulating protein recycling. Indeed, it was previously shown that kinesin II also binds to Rab4 (Imamura et al., 2003), the GTPase that has been shown to regulate fast recycling from early endosomes to the plasma membrane. What causes the accumulation of endosomes at the tips of the cells? Since kinesin II is a plus-directed molecular motor, perhaps one would expect Kif3B knockdown to result in endosome accumulation around the microtubule-organizing complex (MTOC). Interestingly, the tips of the cells that contain accumulated endosomes upon Kif3B knockdown are also rich in actin (data not shown and supplementary material Fig. S7). Recent evidence suggests that the interplay between microtubule motors and actin motors (myosins) is a key regulatory step in determining the transport vesicle sorting and recycling. For instance, in melanocytes myosin Va is required for the capture of melanosomes in actin-rich cell protrusions (Fukuda et al., 2002; Hume et al., 2002; Wu et al., 2002a). The mutation of either myosin Va or its recruiting proteins (melanophilin and Rab27) results in the dispersion of melanosomes in the cytoplasm of the cell (Wu et al., 2002b). Similarly, Myosin Vb associates with recycling endosomes by binding to FIP2 and Rab11 (Hales et al., 2002; Lapierre et al., 2001). Overexpression of myosin Vb dominant-negative inhibitor (MyoVb-tail) results in accumulation of endosomes around the MTOC, presumably because they cannot be captured on the actin-rich cell protrusions (Hales et al., 2002; Lapierre et al., 2001). Thus, kinesin II may be required for the dissociation of endosomes from the actin cytoskeleton. Consistent with this, actin depolymerization inhibited accumulation of endosomes in the cell periphery induced by Kif3B depletion (supplementary material Fig. S7). Furthermore, recent reports, as well as our data, suggest that kinesin II and myosin Vb are present on the same endocytic transport vesicles (Kashina et al., 2004). Interestingly, in contrast to mammalian cells, *Drosophila* cells only have one Class I FIP, which binds to myosin V and is known as dRip11 (Li et al., 2007). This study raises the interesting possibility that in *Drosophila* cells, dRip11 might bind to both molecular motors, myosin V and kinesin II, thus allowing the crosstalk between actin- and microtubule-based endosome transport.

In summary, we propose that internalized TfR can be recycled either via a 'slow' regulated recycling pathway or a 'fast' constitutive recycling pathway, which probably represents direct transport from peripheral early endosomes to the plasma membrane. Our data suggest that Rip11/FIP5 is required for mediating the sorting of proteins to the slow recycling pathway, whereas other FIPs might regulate the recycling from perinuclear recycling endosomes to the plasma membrane or direct transport of proteins from early endosomes to the plasma membrane (Fig. 8D). Rip11/FIP5 functions, at least in part, by binding to kinesin II. Although the exact role of kinesin II in endocytic recycling remains to be fully understood, our data suggest that it mediates the transport of endocytic carriers as well as regulates differential association of recycling endosomes with microtubule and actin cytoskeletons.

Materials and Methods

Antibodies

Rabbit anti-Rip11/FIP5 and rabbit anti-RCP/FIP1 antibodies were previously described (Prekeris et al., 2000; Peden et al., 2004). Mouse anti-kinesin II antibody was purchased from Covance (Berkeley, CA). Anti-KAP3A antibody was obtained from Transduction laboratories (San Diego, CA). Mouse anti-EEA1, mouse anti-transferrin receptor and mouse anti-β-tubulin antibodies were from BD Biosciences (San Jose, CA). Rabbit anti-VAMP3 was purchased from Abcam (Cambridge, MA). Secondary antibodies conjugated to either fluorescein or Texas Red were from Jackson ImmunoResearch (West Grove, PA). Transferrin conjugated to Alexa-Fluor-488 or Alexa-Fluor-594 was purchased from Molecular Probes/Invitrogen (Eugene, OR).

Yeast two-hybrid assays

The bait construct was prepared by subcloning full-length Rip11/FIP5 into the pGBKT7 plasmid. The construct was used to transform AH109 yeast cells according to the manufacturer's protocol (Clontech, Palo Alto CA). A human kidney cDNA library was screened by mating Y187 yeast cells with AH109 cells expressing Rip11/FIP5. Colonies were then checked for growth and β-galactosidase expression by X-gal filter assay. As a further test to eliminate false positives, isolated prey vectors were co-transformed with Rip11/FIP5 or pGBKT7 alone and checked again for reporter gene expression.

For protein interaction studies, a series of bait constructs (in pGBKT7 vector) were constructed using the following cDNAs: RCP/FIP1, Rip11/FIP5-Y629A, Kif3B(524-747)-tail, KAP3. For prey constructs, the following cDNAs were inserted into pACT2 vector: Kif3B, KAP3, Rab11a, Rab11a-S25N, Rab11a-Q70L. The interaction between bait and prey was measured using liquid β-galactosidase assay according to manufacturer's protocol (Clontech, Palo Alto, CA).

Imaging

For imaging, HeLa cells were seeded on collagen-coated coverslips and fixed with 4% paraformaldehyde for 15 minutes. After fixation, cells were permeabilized with phosphate-buffered saline containing 0.4% saponin, 0.2% BSA and 1% fetal bovine serum. Cells were subsequently stained using standard immunofluorescence staining procedures and imaged using an inverted Zeiss Axiovert 200M deconvolution microscope. Images were processed using Intelligent Imaging Innovations (Denver,

CO) three-dimensional (3D) rendering and exploration software. For time-lapse microscopy mock-treated or siRNA-treated HeLa cells were plated on collagen-coated coverslips and incubated with 5 μg/ml of Tf–Alexa-Fluor-488 for 30 minutes at 37°C. Cells were then washed and mounted on PH2 heated platform fitted with a TC-344B dual automatic temperature controller (Warner Instruments) and imaged as described above.

RNA interference

RCP/FIP1 siRNA duplexes were previously described (Peden et al., 2004). siRNA duplexes for Rip11/FIP5 (siRNA1: 5′-GAGCTGAGTGCTCAGGCTATT-3′ and siRNA2: 5′-GGGCTGGAGAAGCTCAAAATT-3′) (Peden et al., 2004) and Kif3B (siRNA1: 5′-GAAATGCATGGGTAAGGTATT-3′ and siRNA2: 5′-CGCTAAGG-TGGGTAGCCTATT-3′) were based on human sequences. To knock down Rip11/FIP5, RCP/FIP1 or Kif3B HeLa cells were transfected with 10 nM HPP grade siRNA (QIAGEN, Valencia, CA) using Lipofectamine 2000 (Invitrogen, Carlsbad, CA) based on manufacturer's protocol. Transfected cells were incubated for 72 hours, plated on collagen-coated coverslips and imaged using fluorescence microscopy or analyzed by immunoblotting and flow cytometry.

Expression constructs and protein purification

mRFP-tagged myosin Vb tail, GST-Rab11a, GST-Rip11(490-652) constructs were described previously (Hales et al., 2002; Meyers and Prekeris, 2002). GST-Kif3A-tail(531-698), GST-Kif3B-tail(524-747), GST-Kif3C-tail(571-793) fusion proteins were created by cloning corresponding cDNA into pGEX-KG plasmid (Amersham Biosciences, Piscataway, NJ) using *Eco*RI and *Xho*I sites. GST-fusion and 6His-fusion proteins were expressed using BL21-RIPL *E.coli* strain or baculovirus expression system as described previously (Junutula et al., 2004; Tarbutton et al., 2005).

Flow cytometry

The Tf- and EGFR-uptake assays were done as previously described (Peden et al., 2004). Briefly, mock- or siRNA-transfected cells were incubated with 10 μg/ml Tf-Alexa488 at 4°C for 30 minutes. Cells were then incubated at 37°C for various time intervals in the continuous presence of either 10 μg/ml Tf-Alexa488. For EGFR uptake, cells were incubated with anti-EGFR-Alexa594 antibody in the presence of 8 ng/ml of EGF. Cells were then washed once with 0.1 M glycine (pH 3.5), followed by two washes with phosphate-buffered saline. The experiment was completed by pelleting and resuspending cells in 3% paraformaldehyde. Cell-associated Tf-Alexa488 or anti-EGFR-Alexa594 antibody were determined by flow cytometry.

For recycling assays, cells were incubated with Tf-Alexa488 for 30 minutes at 37°C. Cells were washed once with 0.1 M glycine (pH 3.5), followed by two washes with phosphate-buffered saline. Cells were then incubated in complete medium supplemented with 50 μg/ml unlabelled Tf at 37°C for various times prior to wash and fixation. Cell-associated Tf-Alexa647 was determined by flow cytometry.

To measure plasma-membrane-associated TfR, HeLa cells were fixed with 3% paraformaldehyde. Cells were then washed and incubated with either 5 μg/ml anti-TfR-Alexa488 antibody or 80 μg/ml Tf-Alexa488 in the presence (to measure total cellular TfR) or absence (to measure plasma membrane TfR) of 0.4% saponin. To measure plasma-membrane-associated EGFR, cells were incubated with anti-EGFR-Alexa594 antibody. Cells were then washed and amount of cell-associated Tf-Alexa488, anti-TfR-Alexa488 or anti-EGFR-Alexa594 antibody were determined by flow cytometry.

DQ-BSA-green degradation assay

To measure the lysosomal degradation of soluble proteins we used a DQ-BSA-green degradation assay. DQ-BSA-green is a BSA labeled with a self-quenching fluorescent dye. The hydrolysis of the DQ-BSA-green into single dye-labeled peptides by lysosomal proteases relieves self-quenching, thus allowing us to measure the lysosomal DQ-BSA-green transport. The assay was done according to the manufacturer's protocol (Molecular Probes/Invitrogen, Eugene, OR). Briefly, mock- or siRNA-treated HeLa cells were loaded with 200 μg/ml DQ-BSA-green for 1 hour at 37°C. Cells were then washed to remove extracellular DQ-BSA-green and incubated at 37°C for 2 hours. The fluorescence of DQ-BSA-green was then monitored by flow cytometry.

Electron microscopy

For immunoelectron microscopy, HeLa cells were incubated with Tf-HRP for 45 minutes at 37°C before being chilled on ice. The HRP-containing compartments were then preserved by performing the DAB reaction prior to digitonin permeabilization, paraformaldehyde fixation and incubation with rabbit anti-Rip11/FIP5, followed by 10 nm gold-conjugated anti-rabbit IgG antibody, essentially as described previously (Futter et al., 1998). Thin sections, 60-70 nm thick, were cut using a Reichert-Jung Ultracut E microtome, stained with lead citrate and viewed in a Phillips CM12 transmission electron microscope. Some additional images were captured using a Morada CCD camera (Olympus Soft Imaging Systems) coupled to a Tecnai G2 Spirit transmission electron microscope (FEI, The Netherlands), running iTEM software.

Microtubule sedimentation assay

Purified tubulin was polymerized as described in the manufacturer's protocol provided in the Microtubule Spin-Down Assay kit (Cytoskeleton, Denver, CO). Briefly, HeLa cells were lysed in reaction buffer (20 mM HEPES, pH 7.4, 10 mM NaCl, 5 mM $MgCl_2$) using 1% Triton X-100. Insoluble material was then sedimented and lysates diluted to 0.1% Triton X-100 and with a final protein concentration of 1 mg/ml. Purified tubulin was polymerized and stabilized with Taxol. 40 μl polymerized microtubules (0.5 mg/ml) were then mixed with 80 μl of cell lysates and 100 μl of reaction buffer containing Taxol. As a negative control, tubulin was not added to one of the reactions. Reactions were then incubated at room temperature for 30 minutes. Where indicated, 20 μg of purified recombinant Kif3B-tail or 5 mM ATP was added. To sediment microtubules, samples were overlaid on 100 μl cushion buffer (reaction buffer with 20% sucrose) and centrifuged at 45,000 r.p.m. for 40 minutes using a TLS55 rotor. Supernatant was aspirated and the supernatant cushion interphase washed with reaction buffer. The microtubule pellet was then resuspended, separated by SDS-PAGE and immunoblotted for the presence of β-tubulin and Rip11/FIP5, Kif3B, TfR or KHC.

KAP3, Kif3A, Kif3B, and Kif3C cDNAs were generous gifts from Tetsu Akiyama (University of Tokyo). This work was supported by NIH National Institute of Diabetes and Digestive and Kidney Disease (NIDDK) Grants R01DK-064380 (to R.P.), R01DK-070856 (to J.R.G.) and R01DK-070856 (to J.R.G.).

References

Bananis, E., Nath, S., Gordon, K., Satir, P., Stockert, R. J., Murray, J. W. and Wolkoff, A. W. (2004). Microtubule-dependent movement of late endocytic vesicles *in vitro*: requirements for Dynein and Kinesin. *Mol. Biol. Cell* **15**, 3688-3697.

Blasius, T. L., Cai, D., Jih, G. T., Toret, C. P. and Verhey, K. J. (2007). Two binding partners cooperate to activate the molecular motor Kinesin-1. *J. Cell Biol.* **176**, 11-17.

Borner, G. H., Harbour, M., Hester, S., Lilley, K. S. and Robinson, M. S. (2006). Comparative proteomics of clathrin-coated vesicles. *J. Cell Biol.* **175**, 571-578.

Brown, C. L., Maier, K. C., Stauber, T., Ginkel, L. M., Wordeman, L., Vernos, I. and Schroer, T. A. (2005). Kinesin-2 is a motor for late endosomes and lysosomes. *Traffic* **6**, 1114-1124.

Casanova, J. E., Wang, X., Kumar, R., Bhartur, S. G., Navarre, J., Woodrum, J. E., Altschuler, Y., Ray, G. S. and Goldenring, J. R. (1999). Association of Rab25 and Rab11a with the apical recycling system of polarized Madin-Darby canine kidney cells. *Mol. Biol. Cell* **10**, 47-61.

Cole, D. G., Cande, W. Z., Baskin, R. J., Skoufias, D. A., Hogan, C. J. and Scholey, J. M. (1992). Isolation of a sea urchin egg kinesin-related protein using peptide antibodies. *J. Cell Sci.* **101**, 291-301.

Cole, D. G., Chinn, S. W., Wedaman, K. P., Hall, K., Vuong, T. and Scholey, J. M. (1993). Novel heterotrimeric kinesin-related protein purified from sea urchin eggs. *Nature* **366**, 268-270.

Eathiraj, S., Mishra, A., Prekeris, R. and Lambright, D. G. (2006). Structural basis for Rab11-mediated recruitment of FIP3 to recycling endosomes. *J. Mol. Biol.* **364**, 121-135.

Fan, J. and Beck, K. A. (2004). A role for the spectrin superfamily member Syne-1 and kinesin II in cytokinesis. *J. Cell Sci.* **117**, 619-629.

Fielding, A. B., Schonteich, E., Matheson, J., Wilson, G., Yu, X., Hickson, G. R., Srivastava, S., Baldwin, S. A., Prekeris, R. and Gould, G. W. (2005). Rab11-FIP3 and FIP4 interact with Arf6 and the exocyst to control membrane traffic in cytokinesis. *EMBO J.* **24**, 3389-3399.

Filipeanu, C. M., Zhou, F., Lam, M. L., Kerut, K. E., Claycomb, W. C. and Wu, G. (2006). Enhancement of the recycling and activation of beta-adrenergic receptor by Rab4 GTPase in cardiac myocytes. *J. Biol. Chem.* **281**, 11097-11103.

Fukuda, M., Kuroda, T. S. and Mikoshiba, K. (2002). Slac2-a/melanophilin, the missing link between Rab27 and myosin Va: implications of a tripartite protein complex for melanosome transport. *J. Biol. Chem.* **277**, 12432-12436.

Futter, C. E., Gibson, A., Allchin, E. H., Maxwell, S., Ruddock, L. J., Odorizzi, G., Domingo, D., Trowbridge, I. S. and Hopkins, C. R. (1998). In polarized MDCK cells basolateral vesicles arise from clathrin-gamma-adaptin-coated domains on endosomal tubules. *J. Cell Biol.* **141**, 611-623.

Grosshans, B. L., Ortiz, D. and Novick, P. (2006). Rabs and their effectors: achieving specificity in membrane traffic. *Proc. Natl. Acad. Sci. USA* **103**, 11821-11827.

Hales, C. M., Griner, R., Hobdy-Henderson, K. C., Dorn, M. C., Hardy, D., Kumar, R., Navarre, J., Chan, E. K., Lapierre, L. A. and Goldenring, J. R. (2001). Identification and characterization of a family of Rab11-interacting proteins. *J. Biol. Chem.* **276**, 39067-39075.

Hales, C. M., Vaerman, J. P. and Goldenring, J. R. (2002). Rab11 family interacting protein 2 associates with Myosin Vb and regulates plasma membrane recycling. *J. Biol. Chem.* **277**, 50415-50421.

Haraguchi, K., Hayashi, T., Jimbo, T., Yamamoto, T. and Akiyama, T. (2006). Role of the kinesin-2 family protein, KIF3, during mitosis. *J. Biol. Chem.* **281**, 4094-4099.

Hickson, G. R., Matheson, J., Riggs, B., Maier, V. H., Fielding, A. B., Prekeris, R., Sullivan, W., Barr, F. A. and Gould, G. W. (2003). Arfophilins are dual Arf/Rab11 binding proteins that regulate recycling endosome distribution and are related to Drosophila nuclear fallout. *Mol. Biol. Cell* **14**, 2908-2920.

Hoekstra, D., Tyteca, D. and van Ijzendoorn, S. C. (2004). The subapical compartment: a traffic center in membrane polarity development. *J. Cell Sci.* **117**, 2183-2192.

Hume, A. N., Collinson, L. M., Hopkins, C. R., Strom, M., Barral, D. C., Bossi, G., Griffiths, G. M. and Seabra, M. C. (2002). The leaden gene product is required with Rab27a to recruit myosin Va to melanosomes in melanocytes. *Traffic* **3**, 193-202.

Imamura, T., Huang, J., Usui, I., Satoh, H., Bever, J. and Olefsky, J. M. (2003). Insulin-induced GLUT4 translocation involves protein kinase C-lambda-mediated functional coupling between Rab4 and the motor protein kinesin. *Mol. Cell. Biol.* **23**, 4892-4900.

Jagoe, W. N., Lindsay, A. J., Read, R. J., McCoy, A. J., McCaffrey, M. W. and Khan, A. R. (2006). Crystal structure of rab11 in complex with rab11 family interacting protein 2. *Structure* **14**, 1273-1283.

Jimbo, T., Kawasaki, Y., Koyama, R., Sato, R., Takada, S., Haraguchi, K. and Akiyama, T. (2002). Identification of a link between the tumour suppressor APC and the kinesin superfamily. *Nat. Cell Biol.* **4**, 323-327.

Jordens, I., Marsman, M., Kuijl, C. and Neefjes, J. (2005). Rab proteins, connecting transport and vesicle fusion. *Traffic* **6**, 1070-1077.

Junutula, J. R., Schonteich, E., Wilson, G. M., Peden, A. A., Scheller, R. H. and Prekeris, R. (2004). Molecular characterization of Rab11 interactions with members of the family of Rab11-interacting proteins. *J. Biol. Chem.* **279**, 33430-33437.

Kashina, A. S., Semenova, I. V., Ivanov, P. A., Potekhina, E. S., Zaliapin, I. and Rodionov, V. I. (2004). Protein kinase A, which regulates intracellular transport, forms complexes with molecular motors on organelles. *Curr. Biol.* **14**, 1877-1881.

Lapierre, L. A., Kumar, R., Hales, C. M., Navarre, J., Bhartur, S. G., Burnette, J. O., Provance, D. W., Jr, Mercer, J. A., Bahler, M. and Goldenring, J. R. (2001). Myosin vb is associated with plasma membrane recycling systems. *Mol. Biol. Cell* **12**, 1843-1857.

Li, B. X., Sotah, K. A. and Ready, D. F. (2007). Myosin V, rab11, and dRip11 direct apical secretion and cellular morphogenesis in developing *Drosophila* photoreceptors. *J. Cell Biol.* **177**, 659-669.

Lin, F., Hiesberger, T., Cordes, K., Sinclair, A. M., Goldstein, L. S., Somlo, S. and Igarashi, P. (2003). Kidney-specific inactivation of the KIF3A subunit of kinesin-II inhibits renal ciliogenesis and produces polycystic kidney disease. *Proc. Natl. Acad. Sci. USA* **100**, 5286-5291.

Lindsay, A. J., Hendrick, A. G., Cantalupo, G., Senic-Matuglia, F., Goud, B., Bucci, C. and McCaffrey, M. W. (2002). Rab coupling protein (RCP), a novel Rab4 and Rab11 effector protein. *J. Biol. Chem.* **277**, 12190-12199.

Maxfield, F. R. and McGraw, T. E. (2004). Endocytic recycling. *Nat. Rev. Mol. Cell. Biol.* **5**, 121-132.

Mellman, I. (1996). Endocytosis and molecular sorting. *Annu. Rev. Cell Dev. Biol.* **12**, 575-625.

Meyers, J. M. and Prekeris, R. (2002). Formation of mutually exclusive Rab11 complexes with members of the family of Rab11-interacting proteins regulates Rab11 endocytic targeting and function. *J. Biol. Chem.* **277**, 49003-49010.

Naslavsky, N., Rahajeng, J., Sharma, M., Jovic, M. and Caplan, S. (2006). Interactions between EHD proteins and Rab11-FIP2: a role for EHD3 in early endosomal transport. *Mol. Biol. Cell* **17**, 163-177.

Nedvetsky, P. I., Stefan, E., Frische, S., Santamaria, K., Wiesner, B., Valenti, G., Hammer, J. A., 3rd, Nielsen, S., Goldenring, J. R., Rosenthal, W. et al. (2007). A role of myosin Vb and Rab11-FIP2 in the aquaporin-2 shuttle. *Traffic* **8**, 110-123.

Peden, A. A., Schonteich, E., Chun, J., Junutula, J. R., Scheller, R. H. and Prekeris, R. (2004). The RCP-Rab11 complex regulates endocytic protein sorting. *Mol. Biol. Cell* **15**, 3530-3541.

Pelissier, A., Chauvin, J. P. and Lecuit, T. (2003). Trafficking through Rab11 endosomes is required for cellularization during Drosophila embryogenesis. *Curr. Biol.* **13**, 1848-1857.

Powelka, A. M., Sun, J., Li, J., Gao, M., Shaw, L. M., Sonnenberg, A. and Hsu, V. W. (2004). Stimulation-dependent recycling of integrin beta1 regulated by ARF6 and Rab11. *Traffic* **5**, 20-36.

Prekeris, R. (2003). Rabs, Rips, FIPs, and endocytic membrane traffic. *ScientificWorldJournal* **3**, 870-880.

Prekeris, R., Klumperman, J. and Scheller, R. H. (2000). A Rab11/Rip11 protein complex regulates apical membrane trafficking via recycling endosomes. *Mol. Cell.* **6**, 1437-1448.

Prekeris, R., Davies, J. M. and Scheller, R. H. (2001). Identification of a novel Rab11/25 binding domain present in Eferin and Rip proteins. *J. Biol. Chem.* **276**, 38966-38970.

Robinson, M. S., Watts, C. and Zerial, M. (1996). Membrane dynamics in endocytosis. *Cell* **84**, 13-21.

Shiba, T., Koga, H., Shin, H. W., Kawasaki, M., Kato, R., Nakayama, K. and Wakatsuki, S. (2006). Structural basis for Rab11-dependent membrane recruitment of a family of Rab11-interacting protein 3 (FIP3)/Arfophilin-1. *Proc. Natl. Acad. Sci. USA* **103**, 15416-15421.

Shin, O. H., Couvillon, A. D. and Exton, J. H. (2001). Arfophilin is a common target of both class II and class III ADP-ribosylation factors. *Biochemistry* **40**, 10846-10852.

Skop, A. R., Bergmann, D., Mohler, W. A. and White, J. G. (2001). Completion of cytokinesis in C. elegans requires a brefeldin A-sensitive membrane accumulation at the cleavage furrow apex. *Curr. Biol.* **11**, 735-746.

Soldati, T. and Schliwa, M. (2006). Powering membrane traffic in endocytosis and recycling. *Nat. Rev. Mol. Cell. Biol.* **7**, 897-908.

Takeda, S., Yamazaki, H., Seog, D. H., Kanai, Y., Terada, S. and Hirokawa, N. (2000). Kinesin superfamily protein 3 (KIF3) motor transports fodrin-associating vesicles important for neurite building. *J, Cell Biol.* **148**, 1255-1265.

Tarbutton, E., Peden, A. A., Junutula, J. R. and Prekeris, R. (2005). Class I FIPs, Rab11-binding proteins that regulate endocytic sorting and recycling. *Meth. Enzymol.* **403**, 512-525.

Ullrich, O., Reinsch, S., Urbe, S., Zerial, M. and Parton, R. G. (1996). Rab11 regulates recycling through the pericentriolar recycling endosome. *J. Cell Biol.* **135**, 913-924.

van der Sluijs, P., Hull, M., Webster, P., Male, P., Goud, B. and Mellman, I. (1992). The small GTP-binding protein rab4 controls an early sorting event on the endocytic pathway. *Cell* **70**, 729-740.

Wang, X., Kumar, R., Navarre, J., Casanova, J. E. and Goldenring, J. R. (2000). Regulation of vesicle trafficking in madin-darby canine kidney cells by Rab11a and Rab25. *J. Biol. Chem.* **275**, 29138-29146.

Ward, E. S., Martinez, C., Vaccaro, C., Zhou, J., Tang, Q. and Ober, R. J. (2005). From sorting endosomes to exocytosis: association of Rab4 and Rab11 GTPases with the Fc receptor, FcRn, during recycling. *Mol. Biol. Cell* **16**, 2028-2038.

Whitehead, J. L., Wang, S. Y., Bost-Usinger, L., Hoang, E., Frazer, K. A. and Burnside, B. (1999). Photoreceptor localization of the KIF3A and KIF3B subunits of the heterotrimeric microtubule motor kinesin II in vertebrate retina. *Exp. Eye Res.* **69**, 491-503.

Wilson, G. M., Fielding, A. B., Simon, G. C., Yu, X., Andrews, P. D., Peden, A. A., Gould, G. W. and Prekeris, R. (2004). The FIP3-Rab11 protein complex regulates recycling endosome targeting to the cleavage furrow during late cytokinesis. *Mol. Biol. Cell* **16**, 849-860.

Wu, X., Wang, F., Rao, K., Sellers, J. R. and Hammer, J. A., 3rd. (2002a). Rab27a is an essential component of melanosome receptor for myosin Va. *Mol. Biol. Cell* **13**, 1735-1749.

Wu, X. S., Rao, K., Zhang, H., Wang, F., Sellers, J. R., Matesic, L. E., Copeland, N. G., Jenkins, N. A. and Hammer, J. A., 3rd (2002b). Identification of an organelle receptor for myosin-Va. *Nat. Cell Biol.* **4**, 271-278.

Yoon, S. O., Shin, S. and Mercurio, A. M. (2005). Hypoxia stimulates carcinoma invasion by stabilizing microtubules and promoting the Rab11 trafficking of the alpha6beta4 integrin. *Cancer Res.* **65**, 2761-2769.

Zhang, X. M., Ellis, S., Sriratana, A., Mitchell, C. A. and Rowe, T. (2004). Sec15 is an effector for the Rab11 GTPase in mammalian cells. *J. Biol. Chem.* **279**, 43027-43034.